

Figure 1: Simplified schematic of the compensated lattice setup

## 1 Compensated optical lattice

Our experiments take place in a compensated simple cubic optical lattice potential, which is formed at the intersection of three orthogonal axes, see Fig. 1. Along each axis, a 1D lattice potential is formed by retro-reflecting a red-detuned Gaussian beam, which results in a sinusoidal intensity pattern.

Overlapped onto each of the lattice beams we have a compensation beam, which is blue-detuned and thus produces a repulsive potential. The compensation beam is not retro-reflected, so it does not form a standing wave potential, see Fig. 1.

The lattice beam that propagates along the  $x$  axis produces a potential of the form

$$V_L(x; y, z) = -s_0 \exp\left[-2\frac{y^2 + z^2}{w_L^2}\right] \cos^2(k_L x) \quad (1)$$

where  $s_0$  is the lattice depth at the center of the potential,  $w_L$  is the lattice beam waist and  $k_L = 2\pi/\lambda_L$  is the wavenumber of the lattice light. The compensation beam that propagates along  $x$  produces a potential

$$V_C(x; y, z) = g_0 \exp\left[-2\frac{y^2 + z^2}{w_C^2}\right] \quad (2)$$

where  $g_0$  is the depth (or rather height since it is repulsive) of the compensating potential, and  $w_C$  is the beam waist of the compensation beam.

The combined potential of lattice plus compensation for the beams propagating along  $x$  is

$$V_{1D}(x; y, z) = V_L(x; y, z) + V_C(x; y, z) \quad (3)$$

The total potential for our simple cubic lattice is given by

$$V_{3D}(x, y, z) = V_{1D}(x; y, z) + V_{1D}(y; z, x) + V_{1D}(z; x, y) \quad (4)$$

In what follows we will first look at general aspects of the potential, using analytic approximations to its shape and considering a zero temperature sample. Then we will use the high-temperature series expansion (HTSE)<sup>1</sup> and the local density approximation (LDA) to study the system in more detail.

---

<sup>1</sup>The HTSE is an analytical solution to the Hubbard model that is valid at high-temperatures. The HTSE is very good for  $T \gg t$  and works down to  $T/t \sim 1.8$ . This solution gives us the thermodynamic quantities (density, double occupancy, entropy per particle, etc.) for a homogeneous system.

## 2 General aspects of the potential

Before we go ahead and deploy the full machinery of the LDA we will discuss some general aspects of the potential.

One of the important things to note is that at each point in space we will, in general, have three different lattice depths, associated with each of the  $x$ ,  $y$ , and  $z$  lattice directions. For this reason the potential is difficult to visualize. To make things simpler, we can consider the potential along the 111 direction, along this direction we have equal lattice depths in  $x$ ,  $y$ , and  $z$ :

$$s_x(r_{111}) = s_y(r_{111}) = s_z(r_{111}) = s_0 \exp\left[-\frac{4r_{111}^2}{3w_L^2}\right] \equiv s(r_{111}) \quad (5)$$

where  $r_{111}$  represents the distance along the 111 diagonal line.

The bottom envelope of the lattice potential along 111 is given by

$$V_{L,\text{env}}(r_{111}) = -3s_0 \exp\left[-\frac{4r_{111}^2}{3w_L^2}\right] \quad (6)$$

An important aspect of a lattice potential is that the energy spectrum exhibits a band structure. The lowest energy of the band,  $E_0$  can be approximated by the zero-point energy of the 3D harmonic oscillator obtained by Taylor expanding the potential at a lattice site. This approximation is only valid for deep lattices ( $\gtrsim 10 E_R$ ) but we will use it here for its simplicity:

$$E_0 = V_{L,\text{env}} + \frac{3}{2}\hbar\omega_0 = V_{L,\text{env}} + 3E_R\sqrt{s/E_R} \quad (7)$$

We can also obtain an expression for the bandwidth,  $W$ , of the lowest energy band valid in the limit of deep lattices [1]:

$$W = 12t = E_R \frac{48}{\sqrt{\pi}} (s/E_R)^{3/4} e^{-2\sqrt{s/E_R}} \quad (8)$$

Notice that the quantities  $E_0$ ,  $W$ ,  $\omega_0$ ,  $s$ , and  $t$  are all position dependent, and thus functions of  $r_{111}$ .

The energy of the first excited band in the lattice corresponds to an excitation along one of the lattice directions, which is an extra  $\hbar\omega_0$  above the lowest band. In Fig. 2 we have plotted the lattice potential envelopes along with the energy boundaries of the lowest band and a line that is representative of the energy in the first excited band. Also indicated in Fig. 2 is the radius,  $r_{1st}$ , at which the energy of the lowest band is equal to the band gap at the origin:

$$E_0(r_{111} = r_{1st}) = E_1(0) \quad (9)$$

In order to stay within the single band approximation of the Hubbard model, our sample needs to have a size that is smaller than  $r_{1st}$ . An analytical expression for  $r_{1st}$  can be obtained from the quadratic expansion of  $E_0$ :

$$r_{1st} = w_L \left[ \frac{E_R \sqrt{s_0/E_R}}{2s_0 - E_R \sqrt{s_0/E_R}} \right]^{1/2} \quad (10)$$

### 2.1 Lattice locking

On occasion we will want to raise the lattice depth suddenly. This will be useful to get the maximum possible Debye-Waller factor when performing Bragg scattering, or to keep the density distribution

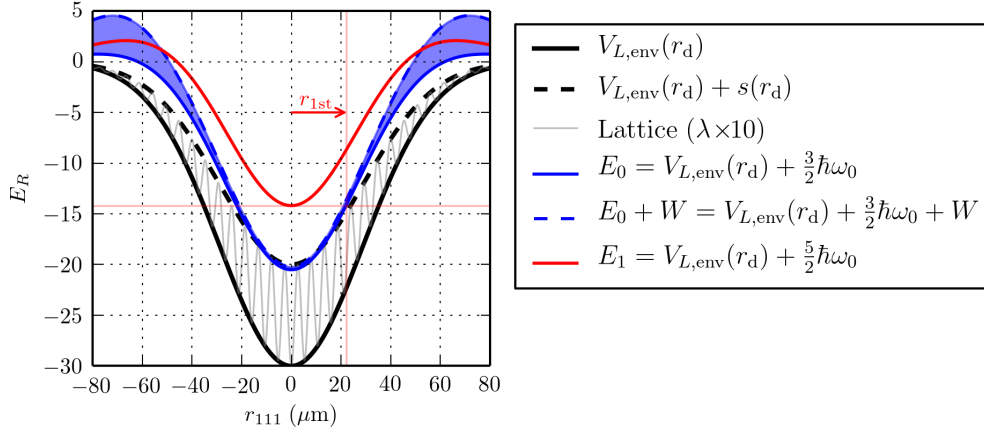


Figure 2: Profiles along  $r_{111}$  for a  $10E_R$  lattice with  $w_L = 47 \mu\text{m}$ .

frozen when sweeping across the narrow Feshbach resonance to make doublons.

For Feshbach sweeps across the narrow resonance we have found that going across from  $80 a_0$  to  $61 a_0$  in 24 ms gives us nearly 100% doublon-to-molecule conversion efficiency. This time can be reduced by a factor of two if we approach the resonance quickly and only slow down the field ramp as we go across it. The time it takes to sweep across the resonance should be much faster than the tunneling time in the locked lattice. We can aim for a factor of five larger tunneling time than sweep time, which for sweep times on the order of 10 ms gives  $t < 20$  Hz. This can be achieved with a lattice depth  $\approx 30 E_R$  as shown in Fig. 3a.

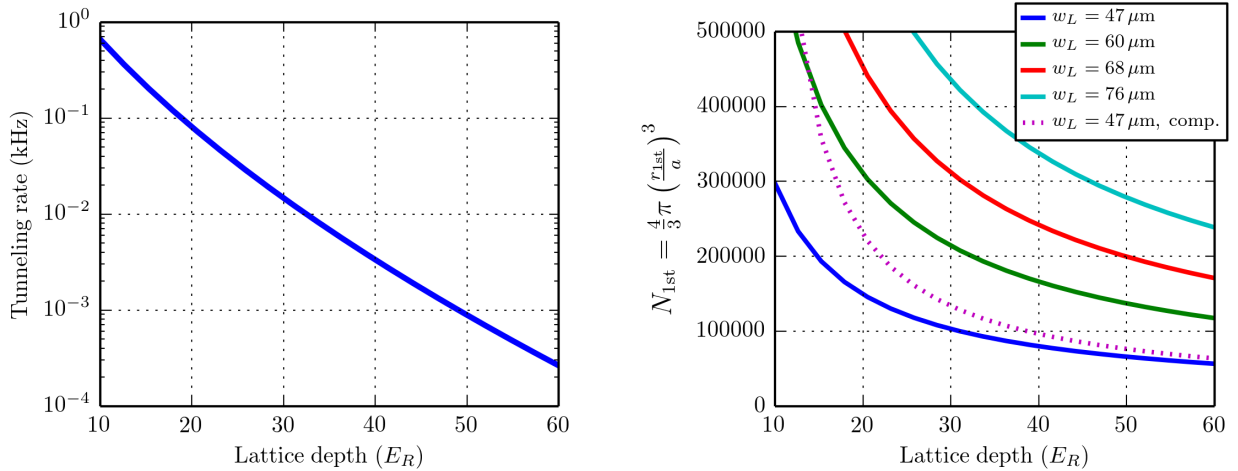
We can use the expression for  $r_{1st}$  in Eq. 10 to estimate of the number of atoms we can hold in a locked lattice without involving higher bands. Assuming a density of one atom per site

$$N_{1st} = \frac{4}{3}\pi \left[ \frac{E_R \sqrt{s_0/E_R}}{2s_0 - E_R \sqrt{s_0/E_R}} \right]^{3/2} \left( \frac{w_L}{a} \right)^3 \quad (11)$$

For a lattice depth  $s_0 = 30 E_R$ ,  $r_{1st} = 0.32w_L$  and  $N_{1st} = 0.13(w_L/a)^3$ . Figure 3b shows a plot of  $N_{1st}$  as a function of lattice depth for various lattice beam waists.

Currently, when doing Bragg scattering measurements, we lock the lattice up to  $20 E_R$  to get the largest possible Debye-Waller factor. In the Bragg experiment we use a compensation of  $3 E_R$  to flatten a  $7 E_R$  lattice and we leave the compensation on as we lock the lattice and probe the sample. Flattening the potential with  $3 E_R$  of compensation results in a maximum atom number of  $\approx 230,000$  atoms to stay in the single band regime with a  $20 E_R$  lock. This is shown with the dotted line in Fig. 3. Our latest experiments with Bragg scattering use an atom number  $N \approx 200,000$ , and we observe that locking the lattice to deeper values, such as  $50 E_R$  and  $80 E_R$  deteriorates our Bragg signals.

Our current lattice waist of  $47 \mu\text{m}$  is an important limitation for our ability to enhance the Debye-Waller factor when doing Bragg scattering or to freeze tunneling to measure the double occupancy. For Bragg we can use compensation to partially compensate the locked lattice, but for double occupancy measurements this is not recommended since the molecules scatter the 532 nm compensation light strongly.



(a) Tunneling rate. The black line is at 2 Hz, which is the rate required to keep the lattice frozen during a measurement of the double occupancy.

(b) Maximum atom number to stay in the single band regime. The dashed line includes  $3 E_R$  of compensation, with a compensation beam waist of  $w_C = 40 \mu\text{m}$ .

Figure 3: Atom number constraints when locking the lattice.

## 2.2 Compensation

Compensation is a way of flattening the profile of the lowest band in order to enlarge the central region of the sample which may exhibit the phase of interest. Using a small lattice beam waist and compensation beams has two important effects [4]:

- The extent of the the phase of interest (Mott state or AFM) in the trapped sample can be enlarged by flattening the potential. A limiting case of this would be a square well potential. With compensation beams the potential can be made quartic instead of quadratic.
- With a small lattice beam waist, the use of compensation enables the possibility of evaporative cooling the sample in the lattice.

With the addition of repulsive compensation beams with depth  $g_0$  and beam waist  $w_C$ , as in Eq. 2, we can expand the lowest band profile of the lattice in a power series as

$$E_0(r_{111}) \approx 3(g_0 + E_R \sqrt{s_0/E_R} - s_0) + \left[ \frac{4s_0 - 2E_R \sqrt{s_0/E_R}}{w_L^2} - \frac{4g_0}{w_C^2} \right] r_{111}^2 + \left[ \frac{-8s_0 + 2E_R \sqrt{s_0/E_R}}{3w_L^4} + \frac{8g_0}{3w_C^4} \right] r_{111}^4 + \mathcal{O}(r_{111}^6) \quad (12)$$

**Enlarging the Mott plateau** If our interest is to maximally flatten the band profile, we see that we can completely cancel the quadratic term in the series expansion by choosing

$$g_0 = \frac{4s_0 - 2\sqrt{s_0}}{4\alpha_w^2} \equiv g_{\text{quartic}} \quad (13)$$

Here we define the beam waist ratio  $\alpha_w = w_L/w_C$  as in [4]. This choice of  $g_0$  will be the most favorable for enlarging the size of the  $n = 1$  region of the cloud, if enough atoms are available to fill up this region.

We point out that, for  $\alpha_w > 1$ , if we use a compensation larger than  $g_{\text{quartic}}$ , the band profile would

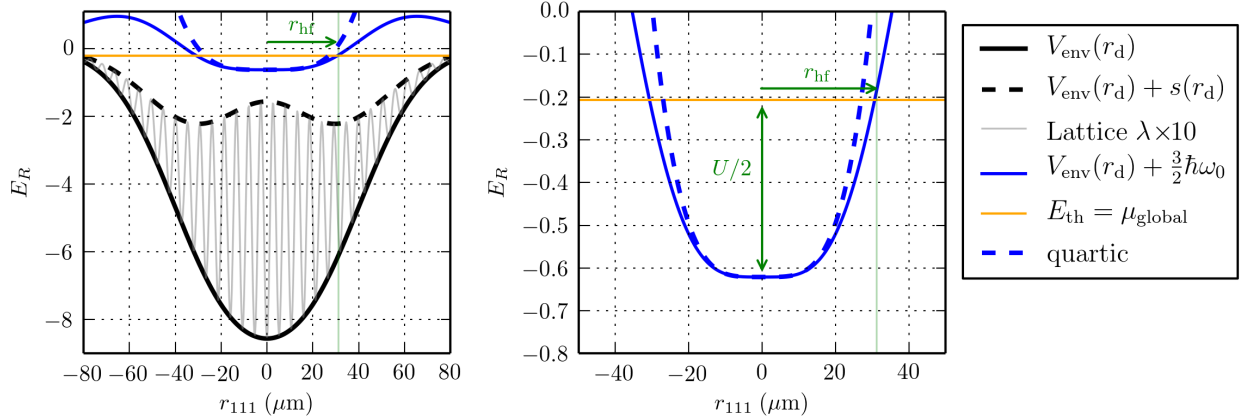


Figure 4: Profiles along  $r_{111}$  for a  $7 E_R$  lattice with  $w_L = 47 \mu\text{m}$ . The compensation is  $g_0 = g_{\text{quartic}}$ , and the chemical potential is set at  $U/2$  to achieve half-filling. This conditions determine the waist ratio  $\alpha_{w,\text{evap}} = 1.17$  such that the chemical potential also matches the evaporation threshold. The figure on the left shows the profile of the lattice potential, which illustrates how the energy scales of the potentials are significantly larger than the energy scales of the Fermi-Hubbard parameters  $U$  and  $t$ . The figure on the right is a zoomed in version of the one on the left.

have a bump in the center. We have observed experimentally that in that case it becomes hard to align the compensation beams such that the sample actually stays at the center of the trap.

In our current experiments we use  $s_0 = 7 E_R$  and our beam waists are approximately  $w_L = 47 \mu\text{m}$  and  $w_C = 40 \mu\text{m}$ , which gives  $\alpha_w = 1.17$ . The necessary compensation to flatten the band would be  $g_{\text{quartic}} = 4.1 E_R$

**Evaporation.** We want to consider the possibility of evaporative cooling in a sample that has  $n = 1$  at the center. To impose  $n = 1$  at the center we set the global chemical potential at  $\mu_{\text{global}} = E_0 + U/2$ , where  $U$  is the on-site interaction strength.

At zero temperature,  $\mu_{\text{global}}$  can be obtained as the value of the band profile at the radius that defines the edge of the cloud. In this way, the  $n = 1$  condition can be written as

$$\mu_{\text{global}} = E_0(r_{\text{hf}}) = U/2 + E_0(0) \quad (14)$$

which defines the radius of the half-filled sample,  $r_{\text{hf}}$ . The situation is illustrated in Fig. 4.

To maximize the evaporation rate for a half-filled sample we need  $E_0(r_{\text{hf}})$  to come as close as possible to the evaporation threshold energy,  $E_{\text{th}}$ . In our setup the threshold is the energy required to escape along one of the lattice beams:

$$E_{\text{th}} = g_0 + E_R \sqrt{s_0/E_R} - s_0 \equiv E_0(0)/3 \quad (15)$$

The evaporation rate is maximized if  $\mu_{\text{global}} = E_{\text{th}}$ . This condition along with Eq. 14, results in

$$E_0(0)/3 = U/2 + E_0(0) \quad \Rightarrow \quad -\frac{2}{3}E_0 = \frac{U}{2} \quad \Rightarrow \quad -2(g_0 + E_R \sqrt{s_0/E_R} - s_0) = U/2 \quad (16)$$

To maximize the size of the Mott plateau we set  $g_0 = g_{\text{quartic}} = \frac{4s_0 - 2\sqrt{s_0}}{4\alpha_w^2}$ . We then solve for the beam

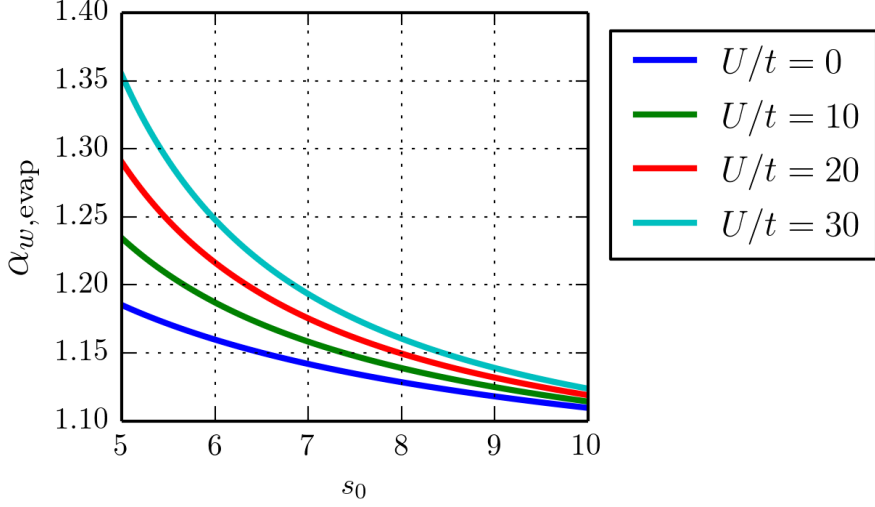


Figure 5: Optimal beam waist ratio for enlarging the central flat portion on the band and maximizing the rate of evaporative cooling.

waist ratio  $\alpha_{w,\text{evap}}$ , which produces the best conditions for evaporation in the lattice:

$$\alpha_{w,\text{evap}}^2 = \frac{4s_0 - 2E_R\sqrt{s_0/E_R}}{4s_0 - 4E_R\sqrt{s_0/E_R} - U} \quad (17)$$

In Fig. 5 we show plots of  $\alpha_{w,\text{evap}}$  for various values of  $U/t$  as a function of lattice depth. We can see that for a  $7 E_R$  lattice  $\alpha_{w,\text{evap}}$  is between 1.15 and 1.20.

We conclude from the analytical considerations presented in this section that a compensated lattice with a value of  $\alpha_w \approx 1.17$  will offer the best scenario for evaporation while flattening the bottom of the band.

### 2.3 Practical considerations

**Atom number** We now turn to examine the number of atoms required in order to achieve half-filling in the optimal setup. To get this number we need to find the half-filling radius,  $r_{\text{hf}}$ , which is defined by Eqs. 14 and 16. Using a density of one atom per site we can obtain the atom number from the radius, as  $N_{\text{hf}} = \frac{4}{3}\pi(r_{\text{hf}}/a)^3$ , where  $a$  is the lattice spacing ( $a = \lambda/2$ ).

To solve for  $r_{\text{hf}}$  we can use the power series expansion of the band energy, which for  $g_0 = g_{\text{quartic}}$  is

$$E_0(r_{\text{hf}}) - E_0(0) = \left[ \frac{2E_R\sqrt{s_0/E_R} - 8s_0 + 4(2s_0 - E_R\sqrt{s_0/E_R})\alpha_w^4}{3w_L^4} \right] r_{\text{hf}}^4 = \frac{U}{2} \quad (18)$$

The solution for  $r_{\text{hf}}$  is then

$$r_{\text{hf}} = \frac{w_L}{\alpha_w} \left[ \frac{3(1 - 2\alpha_w^4 + 2\sqrt{s_0/E_R}(\alpha_w^4 - 1))}{2(1 - 2\alpha_w^4 + 4\sqrt{s_0/E_R}(\alpha_w^4 - 1))} \right]^{1/4} \quad (19)$$

For  $s_0 = 7$  and  $\alpha_w = 1.17$ ,  $r_{\text{hf}} \approx 0.7w_L$ . For a lattice beam waist  $w_L = 47 \mu\text{m}$  this amounts to  $N_{\text{hf}} = 990,000$  atoms. The fully optimized situation for  $w_L = 47 \mu\text{m}$  is shown in Fig. 4.

**Considerations for our current setup** In our current setup we use a lattice depth  $s_0 = 7 E_R$ , and we have approximately  $w_L = 47 \mu\text{m}$  and  $w_C = 40 \mu\text{m}$ , which amounts to  $\alpha_w = 1.175$ . As we have seen above, we should compensate this sample with  $g_{\text{quartic}} = 4.11 E_R$  and populate it with  $N \approx 990,000$  atoms. This would yield a half-filled sample with optimal conditions for evaporative cooling in the lattice.

Unfortunately we only have  $\approx 200,000$  atoms at our disposal. This forces us to reduce the compensation below  $g_{\text{quartic}}$  in order to achieve  $n = 1$  at the center. Reducing the compensation significantly affects the prospects of evaporative cooling in the lattice, but we have no choice since a larger atom number would be problematic for the lattice lock.

The value of  $N = 200,000$  was found empirically to be where the strongest Bragg signals were observed. We can load more atoms into the lattice and use a larger compensation to obtain  $n = 1$ , but our Bragg scattering signal starts getting weaker.

At the moment we use the following compensations for each of the three axes:

axis	1	2	3
$g_0 (E_R)$	3.65	3.90	2.9

With these values we have found empirically that we can obtain the same confinement frequencies in all three directions (which produces spherically symmetric samples) and that we can achieve  $n = 1$  at the center.

### 3 Local density approximation

In the local density approximation (LDA) we consider each point in our potential as an homogeneous system and we set the condition that all of these local homogeneous systems are in thermal equilibrium with each other at some temperature  $T$ . At each point in our potential we can obtain a local value of the lattice depth and the on-site interactions. These two quantities determine the local values of the Hubbard parameters  $t$  and  $U$ . With these in hand, we can use a known solution to the homogeneous Hubbard model and obtain local values for the thermodynamic quantities, such as density, double occupancy, entropy, etc. We can then plot the local thermodynamic quantities as a function of trap position and obtain trap profiles.

An example of the LDA for a uniform lattice potential plus harmonic confinement is shown in Fig. 6. Notice that to obtain the uniform lattice plus confinement we use large values of the beam waists for the lattice and compensation beams, and we use a negative depth for the compensation beam. The resulting trap frequencies in this setup are  $\bar{\nu} = 342 \text{ Hz}$  in all three directions, calculated for  ${}^6\text{Li}$ .

In plots like the one in Fig. 6 we show several lines and regions, and also there are multiple informative labels shown at the top. Below we give the explanation for each of the lines and labels that are shown.

**Parameters of the potential.** The labels on the top left indicate the depth of the lattice and compensating potentials in recoils, and also the waists used for the lattice and compensating beams. The general geometry of the potential is described in §1. Also shown are the beam waist ratio,  $\alpha_w$  and the confinement frequency  $\bar{\nu}$ , which is calculated from the curvature of the bottom of the lowest band.

**Hubbard parameters.** The labels on the top right of the main plot indicate the scattering length and the resulting Hubbard paraemters for the given the lattice depth. The values of  $U/t$ ,  $T/t$ , and  $t$  given are valid at the center of the sample. Due to the finite lattice beam waist the tunneling increases

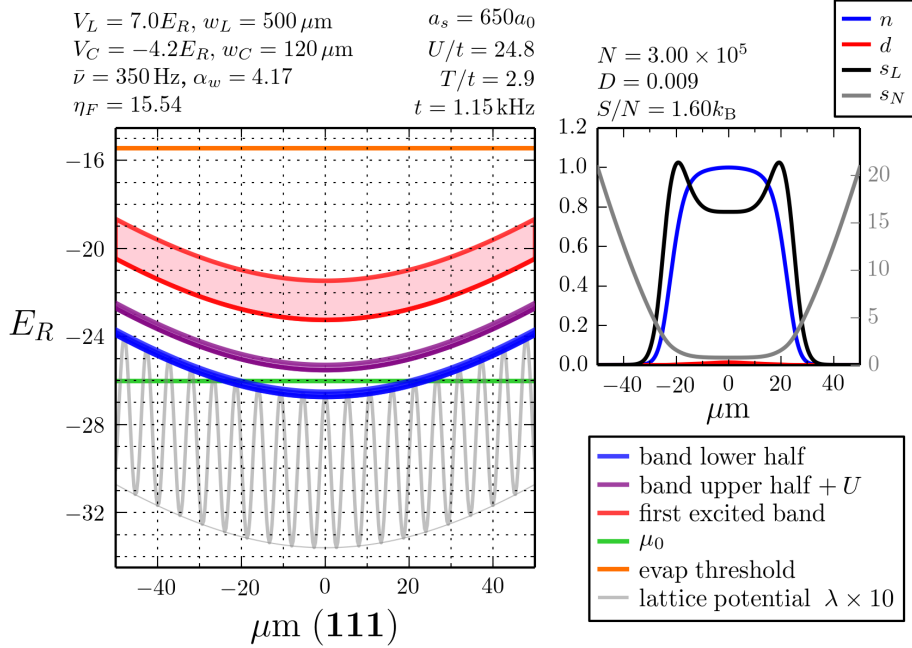


Figure 6: Red detuned uniform lattice with additional harmonic confinement. The confinement is adjusted so that the density is one per site at the center with  $N = 300,000$  atoms. The temperature is adjusted such that the overall entropy per particle is  $S/N = 1.6k_{\text{B}}$ .

as one moves away from the center, and so  $U/t$  and  $T/t$  decrease monotonically for larger distance from the center.

**Band lower half.** This region is defined by two lines, the bottom line corresponds to the lowest energy level accessible to a single particle in the local Hubbard hamiltonian. The top line corresponds to the energy level exactly in the center of the lowest energy band. In the absence of interactions, the Hubbard hamiltonian for a single particle is simply

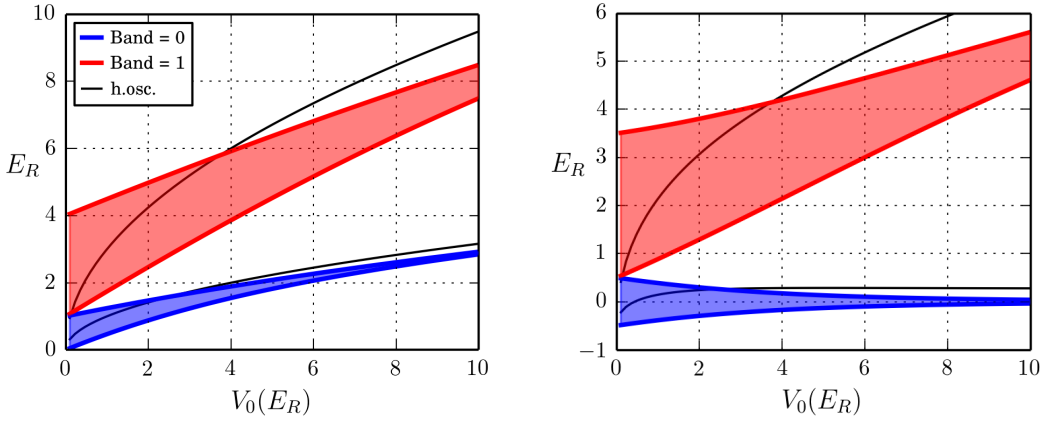
$$H = -\frac{\hbar^2}{2m} \frac{\partial}{\partial x^2} + V_0 \sin^2(kx) \quad (20)$$

The energy level structure as a function of lattice depth is as shown in Fig 7a. In second quantized form the hamiltonian (without interactions) is usually written as

$$H = -t \sum_{\langle ij \rangle, \sigma} a_{i\sigma}^\dagger a_{j\sigma} \quad (21)$$

What is typically not mentioned is that writing the hamiltonian as in Eq. 21 implies a lattice-depth-dependent shift of the energy zero, such that the band structure looks like in Fig. 7b. When solving the Hubbard model using the HTSE we used the hamiltonian in Eq. 21, so energies like the chemical potential are referenced from the center of the lowest band. Most importantly, the center of the lowest band is a ubiquitous energy in the Hubbard model because states below that energy will be almost unperturbed by interactions, whereas states above that energy will be affected significantly by interactions.

**Band upper half +  $U$ .** As we just pointed out in the last paragraph, the states above the center of the lowest band will be modified significantly by the interactions. These states will acquire an extra



(a) Band structure when the zero of energy is at the bottom of the lattice sites. The zero of energy does not change with lattice depth, and the band energies go up almost like the harmonic oscillator state in an individual lattice site.

(b) Band structure when the zero of energy is at the center of the lowest band. This shift is implicit when the hamiltonian is written in second quantized form as in Eq. 21.

Figure 7: Band structure in the Hubbard model.

energy  $U$ , this can be seen for instance if we solve the Hubbard model

$$H = -t \sum_{\langle ij \rangle, \sigma} a_{i\sigma}^\dagger a_{j\sigma} + U \sum_i n_{i\uparrow} n_{i\downarrow} - \mu \sum_{i,\sigma} n_{i,\sigma} \quad (22)$$

in a two-lattice system at half-filling. The solution to this hamiltonian, using exact diagonalization is shown in Fig. 8. It can be seen that the two lower energy levels suffer little change as the interaction are increased, whereas the two higher energy levels are shifted upwards by  $U$ .

The region in the plot called **band upper half +  $U$**  represents the energy levels in the upper half of the lowest band shifted up by the interactions. Of course, this simple picture is not correct in the interacting many-body system but it provides a good representation of what is going on. The separation  $U$  between the band lower half and the band upper half can be used as a measure of the Mott gap.

**First excited band.** This region is simply bounded by the lowest and highest energies in the first excited band. For this band we do not apply shifts due to interactions. This band is primarily shown so that, at a glance, one can asses whether or not the system is in the single band Hubbard regime.

**Global chemical potential.** Denoted by  $\mu_0$ . A fixed global chemical potential is set across the cloud. The local chemical potential is obtained by looking at the separation between  $\mu_0$  and the local zero of energy. We remind the reader that the local zero of energy is the point at the center of the lowest band, i.e. the upper boundary of the blue shaded region.

**Evaporation threshold.** This is the energy required to escape along one of the lattice beams. It is calculated by looking at the profile of the lowest energy level along the 100 direction and finding its maximum. In most cases the maximum will be at infinity, but for  $\alpha_w < 1$  the lowest energy profile along 100 can have a local maximum. In such cases the local maximum is used.

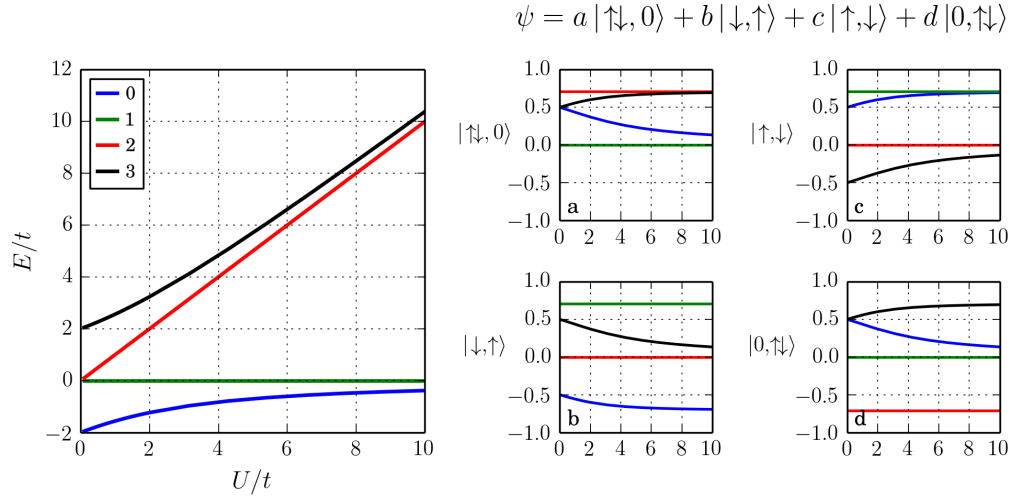


Figure 8: Exact diagonalization solution for the Hubbard hamiltonian, Eq. 22, at half-filling. Notice that the basis states used are second quantized states, so they are already antisymmetrized. For large  $U$  the ground state wavefunction is approximately  $\psi = \frac{1}{\sqrt{2}}(|\uparrow\downarrow\rangle - |\downarrow\uparrow\rangle)$ . This state cannot be written as a Slater determinant because it is an entangled state. For a large number of particles the massive entanglement in the ground state is what makes strongly correlated systems hard to deal with.

**Figure of merit for evaporative cooling in the lattice ( $\eta_F$ ).** When evaporative cooling a thermal gas of atoms, one considers the parameter  $\eta = U_{\text{trap}}/k_B T$ , where  $T$  is the temperature of the gas, and  $U_{\text{trap}}$  is the energy threshold for a particle leaving the trap (i.e. the trap depth) measured with respect to the lowest single-particle energy state. The evaporation rate is suppressed by a factor  $\exp(-\eta)$  where typically  $\eta \sim 10$  and, as the gas cools down, the trap depth is reduced to force further evaporation [9].

For a deeply degenerate Fermi gas,  $T \ll T_F$ , the evaporation rate is given by [9].

$$\Gamma_{\text{evap}} \propto \gamma_{\text{coll}} \frac{T}{T_F} \exp \left[ -\frac{U_{\text{trap}} - k_B T_F}{k_B T} \right] \quad (23)$$

where  $\gamma_{\text{coll}}$  is the classical collision rate evaluated at the Fermi surface. This can also be written as

$$\Gamma_{\text{evap}} \propto \gamma_{\text{coll}} \frac{T}{T_F} \exp \left[ \frac{1}{T/T_F} \right] \exp \left[ -\frac{1}{T/T_F} \left( \frac{U_{\text{trap}}}{k_B T_F} \right) \right] \quad (24)$$

We define  $\eta_F \equiv U_{\text{trap}}/k_B T_F$  and observe that

$$\Gamma_{\text{evap}} \propto \gamma_{\text{coll}} \frac{T}{T_F} \exp \left[ -\frac{\eta_F - 1}{T/T_F} \right] \quad (25)$$

We see that for a given value of  $T/T_F$ , the evaporation rate depends only on  $\eta_F$ . The effective  $\eta$  factor which determines the exponential suppression of the evaporation due to the trap depth is given by

$$\exp(-\eta_{\text{eff}}) = \frac{T}{T_F} \exp \left[ -\frac{\eta_F - 1}{T/T_F} \right] \quad (26)$$

Besides the Boltzmann exponential suppression, the evaporation rate is additionally suppressed by a factor  $T/T_F$  due to Pauli blocking of one of the final states of a collision, which occurs for  $T \ll T_F$  [9]. For a value of  $T/T_F = 0.1$  to get  $\eta_{\text{eff}} = 10$  we need  $\eta_F = 1.77$

**Lattice potential** This line shows a representation of the modulation produced by the lattice potential. The period of the modulations shown is arbitrary and only for illustration purposes. A thin line is also plotted showing the envelope of the lattice potential.

**Trap profiles of thermodynamic quantities.** The smaller plot on the top left corner on Fig. 6 shows the trap profiles of the thermodynamic quantities. It includes the density ( $d$ ), double occupancy ( $d$ ), entropy per lattice site ( $s_L$ ) and entropy per particle ( $s_N$ ). The entropy per particle is shown on the right side axis.

**Overall values of the thermodynamic quantities.** The labels on the top left of the the smaller plot indicate the overall trap values of the thermodynamic quantities that can be obtained by integrating the local values across the volume of the trap.

Now that we have explained the relevant profiles and quantities that can be obtained from the LDA we will use it to get some insight on the idea of entropy redistribution and the possibility of evaporative cooling in the lattice. In the next section we will show how to quantify the entropy capacity of a certain trap configuration. After that we will explore the parameter space and will study the compromise between  $\eta_F$  (the figure of merit for evaporative cooling) and the entropy capacity, keeping in mind that the experiment is constrained by the number of atoms that can be cooled down to  $T/T_F < 0.05$  in the harmonic trap.

### 3.1 Entropy redistribution

In the quest for producing an antiferromagnetically (AFM) ordered state with cold atoms, the entropy per particle,  $S/N$ , is an important metric. It determines the number of quantum states that are accessible to each atom. At half-filling there is an average of one-particle per site<sup>2</sup>. If the temperature of the system is high,  $T \gg U$ , there is an equal probability for a site to be empty, singly or doubly occupied. If the site is singly occupied, the spin there could be up or down, so at high temperatures there are a total of four ( $|0\rangle, |\uparrow\rangle, |\downarrow\rangle, |\uparrow\downarrow\rangle$ ) equally probable state at each lattice site, giving an entropy per particle<sup>3</sup> equal to  $s/k_B = \ln 4 = 1.38$ .

When the temperature is  $T \ll U$ , double occupancies and vacancies are suppressed and the system enters the Mott insulating state. In this case the probability of having empty sites or doubly occupied sites goes to zero. At each site, a particle can still be spin-up or spin-down with equal probability, so the entropy per particle becomes  $s/k_B = \ln 2 = 0.69$ .

As the temperature of the system goes below the Néel temperature, the spin of the atoms becomes strongly determined by their position in the lattice, as they start to order antiferromagnetically. At zero temperature each site has only one possible quantum state (spin-up or spin-down depending on the lattice site) and the entropy per particle goes to zero.

For a homogeneous 3D lattice, at the Néel temperature  $T_N = 0.36t$ , the entropy per particle is  $s = 0.4 k_B$ . As the temperature starts dropping below  $T_N$  the entropy approaches zero very quickly in what is referred to as the AFM transition (AFM stands for antiferromagnetic order). The AFM transition has been studied theoretically for homogeneous 3D systems using quantum Monte Carlo (QMC) [5] and

---

<sup>2</sup>Notice that half-filling corresponds to  $n = 1$ , for this reason sometimes the terms half-filling, unit filling, and unit density are used interchangeably. Here we will restrict the terminology to half-filling or we will write explicitly  $n = 1$  to avoid confusion.

<sup>3</sup>Notice that at half-filling any quantity per particle is the same as per lattice site, since  $n = 1$

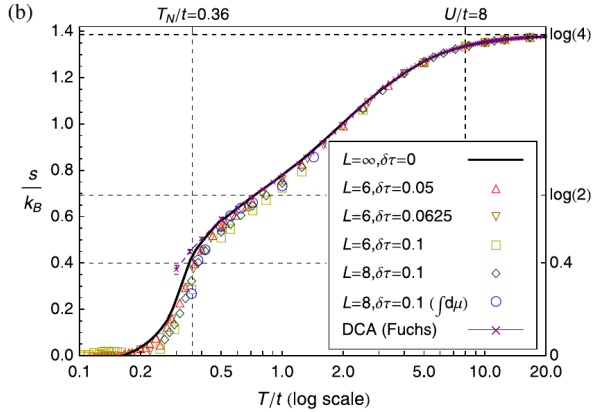


FIG. 1 (color online). (a) Energy per site of homogeneous system at half filling and  $U/t = 8$ , calculated by using DQMC down to  $T/t = 0.1$ . Statistical error bars are smaller than symbols. The solid curve is the entropy extrapolated to  $L = \infty$  and  $d\tau = 0$  (details in Ref. [11]). (b) Entropy per site obtained by integrating down from  $T = \infty$ , showing a shoulder at the Mott scale  $T_{\text{Mott}} \approx U$  and a distinct feature at the Néel temperature  $T_N \approx 0.36t$  due to critical fluctuations. Errors in  $E/t$  and  $s/k_B$  are both about 0.02. Our extrapolated results are fully consistent, within error bars, with the DCA results from Fuchs *et al.* [6].

(a) Paiva [5]

Figure 9: Calculations of entropy per lattice site versus temperature at half filling.

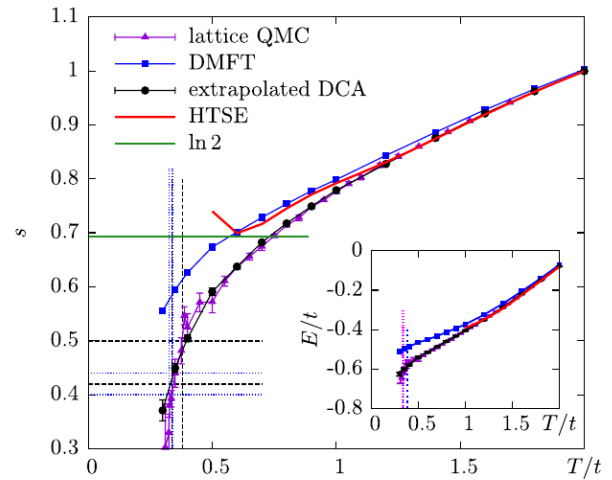


FIG. 1 (color online). Entropy per lattice site  $s$  of the Hubbard model as a function of temperature  $T/t$ , for  $U/t = 8$ , at half filling. Dashed vertical lines (black):  $T_N$  from Ref. [20]; dotted lines (blue): according to DMC simulations. Dashed horizontal lines (black): entropy per lattice site  $s$  at  $T_N$  [20]; dotted lines (blue): according to DMC simulations;  $\log(2)$  is shown as a solid (green) horizontal line. Inset: Energy  $E/t$  per lattice site. The DMC data were extrapolated linearly in  $1/L$  from the data at  $L = 6, 8, 10$ .

(b) Fuchs [6]

the dynamical cluster approximation (DCA) [6]. The results from these two approaches are shown in Figs. 9a,9b.

The theoretical calculations shown correspond to a homogeneous system, but in practice one has samples with a finite number of atoms so one is forced to confine them in order to reach half-filling. Since the confinement is typically harmonic (as opposed to a well with hard walls), the density decays as a function of distance to the center. The inhomogeneity in the density leads to the concept of entropy redistribution. As a consequence, the overall entropy per particle necessary to achieve a Néel state can be higher in a trapped system than in the homogeneous case [5].

### 3.1.1 High temperature series expansion for the Hubbard model

The high temperature series expansion (HTSE) to second order [7, 3] allows us to visualize the properties of the Hubbard model. It works well to capture the properties of the Mott insulating state, however it fails below temperatures of  $T/t \approx 1.8$ , so the AFM state is beyond its reach.

The signatures of the Mott insulating states can be seen in the HTSE solutions shown in Fig. 10, namely:

- The density as function of chemical potential has a plateau at  $n = 1$ , Fig. 10a.
- The double occupancy is suppressed for lower temperatures, Fig. 10b.
- The density fluctuations are suppressed, Fig. 10c.
- The entropy per site as a function of filling has a dip at  $n = 1$ , Fig. 10d.

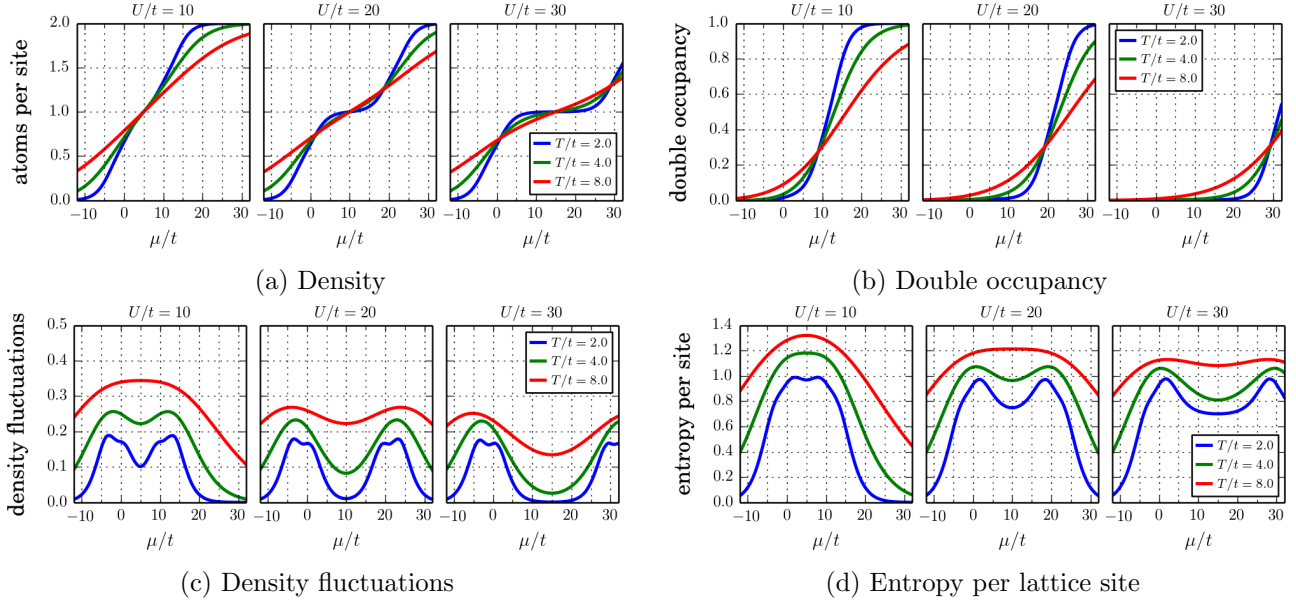


Figure 10: Thermodynamic quantities as a function of chemical potential calculated using the HTSE.

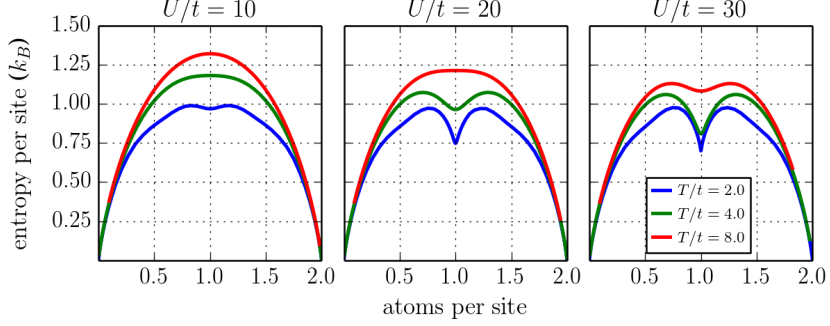


Figure 11: Entropy per lattice site versus density.

### 3.1.2 Entropy per particle

The HTSE gives us the result for the entropy per lattice site, which we can plot versus the density, as shown in Fig. 11. The interesting result arises if we divide the entropy per lattice site by the density, in order to obtain the entropy per particle. This is shown in Fig. 12. It is seen there that the entropy per particle rises significantly for lower filling values, and most importantly that the value of the entropy per particle at low filling **does not** depend strongly on temperature or interaction strength.

In a finite trapped system which inevitably has a shell with density  $n < 1$ , a large part of the total entropy of the system is carried by particles in the shell. This allows the core to be at an effectively lower entropy per particle. At a lower entropy per particle the core can enter the AFM state even if the overall value of  $S/N$  for the entire trap is larger than the Néel entropy of the homogeneous system,  $s_{\text{Néel}} = 0.4k_B$ . A QMC calculation shows that  $S/N = 0.65k_B$  may be low enough to reach an AFM state at the core of the sample. If the sample is loaded adiabatically from a harmonic trap into the lattice this entropy per particle corresponds to  $T/T_F = 0.06$  in the harmonic trap.

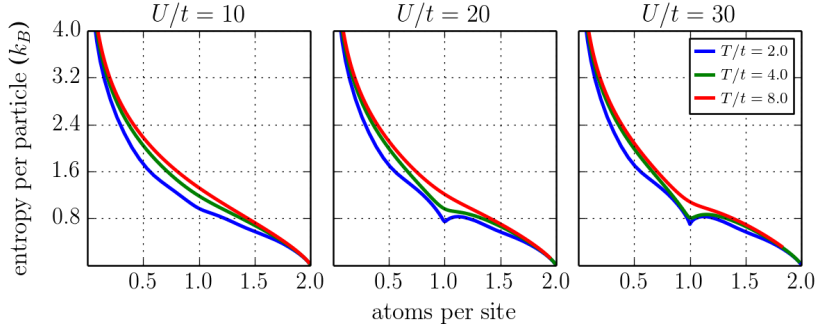


Figure 12: Entropy per particle versus density.

### 3.1.3 Comparing entropy redistribution scenarios

We can consider compensated lattice setups with different beam waist ratios  $\alpha_w$  and different compensation values and determine which setup offers the best scenario for entropy redistribution. There are two approaches to do this. One can realize the LDA at a fixed value of  $S/N$ , find out the resulting temperature of the sample and compare the different scenarios. Alternatively one can realize the LDA at a fixed temperature and compare the values of  $S/N$  for different scenarios.

The first method is more closely related to experiments, because ultracold atoms are isolated systems and the loading of atoms into the lattice should, in principle, proceed adiabatically. In this way one can see for different setups how will the system be adiabatically heated or cooled as it is loaded into the lattice. Since the entropy is a monotonic function of the temperature the second approach, which realizes the LDA at fixed temperature and compares the resulting  $S/N$  is also valid. This approach is easier to implement in the computer code, since the solution to the HTSE is obtained from the grand canonical partition function, which assumes the system is at fixed temperature.

## 4 LDA Results

### 4.1 Optimization of the evaporation figure of merit

We run the LDA for different values of the lattice and compensation beam waists. For each pair of  $w_L$  and  $w_C$  values we minimize the value of  $\eta_F$  by adjusting the compensation depth  $g_0$ . The following constraints are enforced:

- The global chemical potential is set at  $U/2$  to enforce  $n = 1$  at the center of the sample.
- The lowest band is required to have a positive curvature at the origin.
- The resulting density profile is required to decrease monotonically as a function of distance from the center.
- The chemical potential is restricted to be below the energy required for an atom to move along a beam. The purpose of this restriction is to avoid having atoms residing along the lattice beams outside of the beam intersection region. Since we do the LDA at a non-zero temperature, this restriction is implemented as

$$\mu + T < E_{\text{th}}$$

where  $E_{\text{th}}$  is the energy required for an atom to escape along the beams.

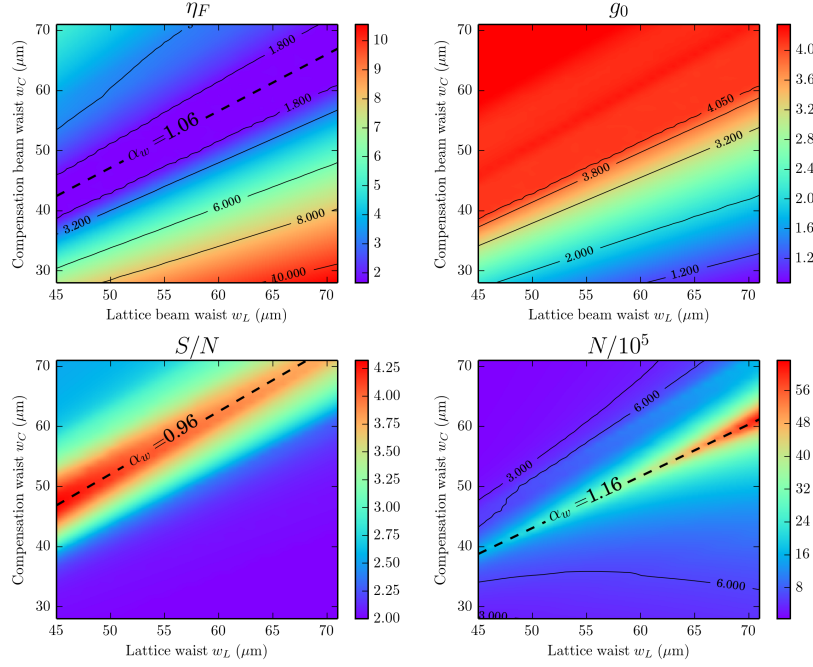


Figure 13: LDA results for the optimization of the evaporation figure of merit  $\eta_F$ . The calculation was performed at a temperature of  $T = 0.4 E_R$ , which for a  $7 E_R$  lattice corresponds to  $T = 10.1t$  at the center. The interactions are set at  $650 a_0$  which is  $U/t = 24.8$  at the center.

Once the value of the compensation is set to minimize  $\eta_F$  the system is defined and we can look at the number of atoms required to realize it and also at the value of  $S/N$ , to assess the capability that the particular configuration has to redistribute the entropy. The results of this optimization are shown in Figs. 13 and 14.

## Observations.

- For  $\alpha_w < 1.16$  the value of green compensation is fixed at  $g_0 \approx 4.1 E_R$ . This means that for  $\alpha_w < 1.16$  the potential can always be compensated such that the chemical potential nearly gets to the energy required to escape along a beam. For  $\alpha_w \ll 1.16$  the lowest energy along a beam direction (say 100) will have a local maximum. Based on our constraints we restrict the compensation such that the chemical potential does not reach the asymptotic energy value along a beam.  $\eta_F$  will then become larger because it is measured with respect to the local maximum (threshold for evaporation) instead of with respect to the asymptotic energy value along the beam. Aside from this aspect, whenever the compensation is  $\approx 4.1 E_R$  we see that  $\eta_F$  attains the lowest value of  $\approx 1.8$ , which is determined by the temperature used in the calculation (at zero temperature  $\eta_F = 1$  would be achieved). The temperature we have used in Fig. 13 is  $T = 0.4 E_R$ , which for a  $7 E_R$  lattice amounts to  $T = 10.1t$  at the center. In Fig. 14 results are shown for  $T = 0.2 E_R$  ( $T = 5.1t$ ), but a region of the parameter space has to be excluded at this temperature. The interactions used are  $a_s = 650 a_0$ , which give  $U/t = 24.8$  at the center of the sample.

A particular aspect of systems with small beam waist is that as one moves away from the center the lattice depth decays and  $t$  gets larger. For a fixed value of  $T$ , then  $T/t$  gets smaller as one moves away from the center. We set  $T/t = 10.1$  at the center so that near the edge we are still at  $T/t > 1.8$  and the HTSE solution to the Hubbard model is still applicable.

- For  $\alpha_w = 1.16$  the sample is flattened optimally with the choice of compensation that also minimizes

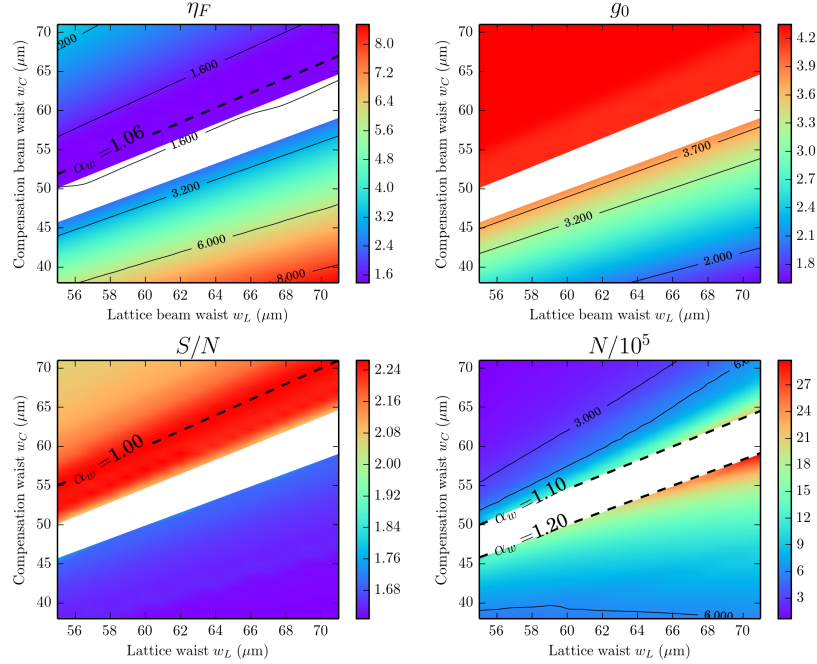


Figure 14: LDA results for the optimization of the evaporation figure of merit  $\eta_F$ . The calculation was performed at a temperature of  $T = 0.2 E_R$ , which for a  $7 E_R$  lattice corresponds to  $T = 5.1t$  at the center. In order to achieve lower temperatures we did not cover the region with optimal compensation from  $\alpha_w = 1.10$  to  $1.20$ . At an optimal compensation the radius of the sample is a large fraction of the beam waist and the value of  $T/t$  at the edge of the cloud is out of reach for the HTSE. The interactions are set at  $650 a_0$  which is  $U/t = 24.8$  at the center.

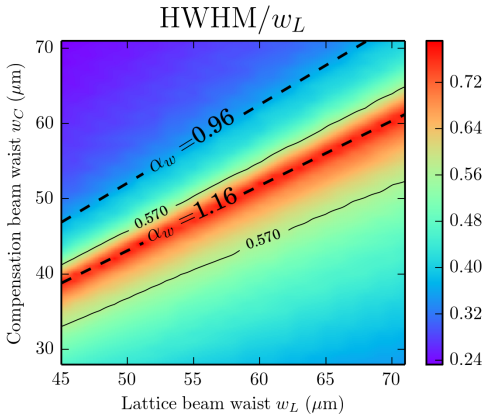


Figure 15: For the same LDA calculation shown in Fig. 13, this plot shows the ratio of the density profile’s half-width at half-max to the lattice beam waist  $w_L$ . This shows that for an optimally flattened sample, you need to fill up a large fraction of your beams in order to reach a chemical potential that is favorable for evaporation. This is why an optimally flattened sample,  $\alpha_w = 1.16$ , with  $w_L = 50 \mu\text{m}$  requires a similar number of atoms than a sample with  $\alpha_w = 1.10$  and  $w_L \approx 70 \mu\text{m}$ .

$\eta_F$ . We obtained nearly the same result analytically in §2.2. Optimal flattening means that one can accomodate a large amount of atoms in the potential. If the atoms are available in the experiment this is a good feature because flattening also means that the extent of the phase of interest at the core of the sample will me maximized. Unfortunately the atom numbers required to reach this regime are beyond the atom number that we can produce in deeply degenerate samples in our experiment. It is tru that using a larger beam waist can most likely enhance the number of atoms that our experiment can produce in deeply degenerate samples, but we expect this number to be less than  $8 \times 10^5$  limited by the atoms that can be evaporated in the ODT and the efficiency of loading them into the dimple potential.

- For  $\alpha_w < 1.16$ , where  $g_0$  can be saturated up to  $4.1 E_R$  to reach an optimal  $\eta_F$ , we can turn to our second important figure of merit: the entropy capacity of the configurution. We see that a value of  $\alpha_w = 0.96$  gives an optimal entropy capacity, since it maximizes  $S/N$  for fixed temperature.
- For a fixed lattice beam waist we see that we can obtain an optimized  $\eta_F$  near 1.8 with a lower atom number if we keep increasing the compensation beam waist. This seems counterintuitive at first because the first thought is that to reach an optimal value of  $\eta_F$  one must fill up the lattice beams up some fraction of their waist. The important point is that the fraction of the waist depends on compensation. If the lattice is flattened optimally then one needs to go far into the lattice beams in order to get the chemical potential to come close to the threshold. If the lattice is just pushed upwards by the compensation but not flattend ( this becomes the case as  $\alpha_w$  moves below 1.16 ) then the fraction of the waist you need to fill up to move the chemical potential close to the threshold is much smaller.

In Fig. 15 we show the fraction of the lattice beam waist that is filled up by the density distribution. For an optimally compensated sample at  $\alpha_w = 1.16$  the fraction can be as large as 0.72 , but for  $\alpha_w = 0.96$  where the entropy capacity of the system is maximized it can be as low as 0.47.

- In conclusion, if we use a lattice ratio  $\alpha_w = 0.96$  we can find a compensation value that allows us to be at half-filling ( $n = 1$  at the center), optimize the evaporation figure of merit ( $\eta_F$  as close as possible to 1) and optimize the entropy capacity of the system ( $S/N$  maximized for fixed temperature) all at the same time. At  $\alpha_w = 0.96$  the optimal setup has a cloud radius that is only

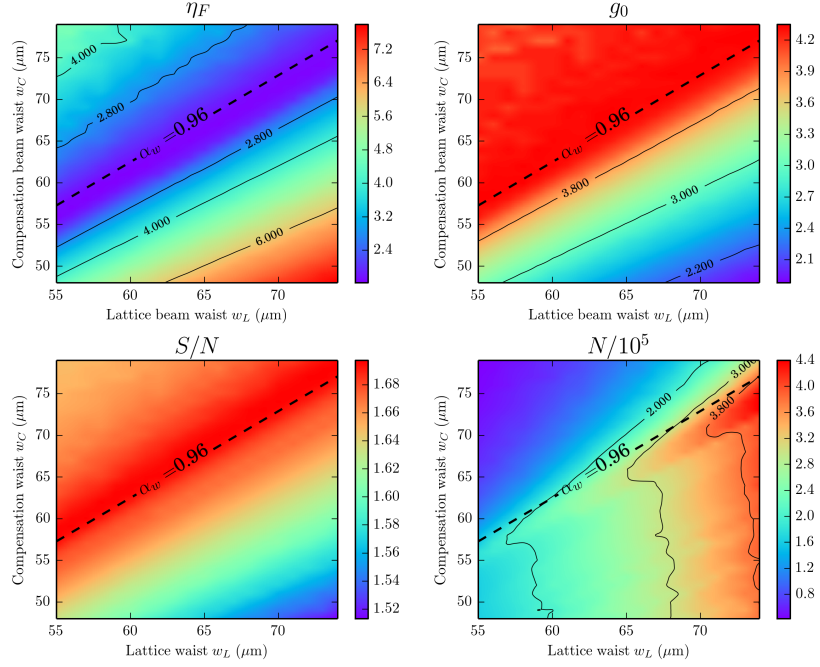


Figure 16: LDA results. At each value of  $w_L$ ,  $w_C$  the compensation is adjusted so that the radius of the sample is  $0.32 w_L$ . Calculation performed at  $T = 0.12 E_R$  which amounts to  $T = 3t$  at the center of the  $7 E_R$  lattice.

$\approx 0.47w_L$ . For a half-filled sample a crude estimate of the atom number can be obtained as

$$N = \frac{4}{3}\pi \left(\frac{r_{\text{cloud}}}{a}\right)^3 = \frac{4}{3}\pi \left(\frac{0.47w_L}{a}\right)^3$$

so a reasonable value of  $N = 500,000$  would require a lattice beam waist  $w_L = 55 \mu\text{m}$ .

As was shown in §2.1 and Fig. 3b a lattice beam waist of  $55 \mu\text{m}$  would only allow us to lock a sample of 500,000 atoms to a depth of  $\approx 10 E_R$ . In order to satisfy the requirements of the lattice lock we will need to compromise on one of our figures of merit.

## 4.2 Lattice locking requirements

Figure 3b shows us that, with large atom numbers, we need to have very big lattice beam waists in order to be able to freeze tunneling and stay in the single band regime. The analytical result shows that to successfully lock a sample up to  $30 E_R$  its radius has to be  $0.32 w_L$ .

We perform an LDA calculation where, for a half-filled sample ( $n = 1$  at the center), we vary the value of the green compensation such that the radius of the sample is equal to  $0.32 w_L$ . The results are shown in Fig. 16, which was calculated at a temperature  $T = 0.12 E_R$  ( $T = 3.0t$ ).

### Observations.

- With  $\alpha_w \approx 0.96$  the best values of both  $\eta_F$  and  $S/N$  can be achieved for a sample that has HWHM =  $0.32 w_L$ , and this is lockable up to  $30 E_R$ . Attaining this with  $N = 300,000$  atoms requires a lattice beam waist  $w_L = 68 \mu\text{m}$ .

- Reducing the compensation to satisfy the locking requirements sets the best  $\eta_F$  and  $S/N$  at  $\eta_F \approx 1.8$  and  $S/N \approx 1.7$  (for  $T = 3t$  at the center).
- $\eta_F$  and  $S/N$  can be optimized independently at  $\alpha_w = 1.06$  and  $\alpha_w = 0.96$  respectively as was shown in the previous section. When setting the radius at  $0.32 w_L$  both  $\eta_F$  and  $S/N$  are optimized almost simultaneously for  $\alpha_w \approx 0.96$ .

### 4.3 Resulting profiles

Below we plot the resulting LDA profiles to further illustrate some of the results obtained above and motivate our conclusions for the future improvements of the setup.

- We start out by showing our current setup,  $w_L = 47 \mu\text{m}$ ,  $w_C = 40 \mu\text{m}$  with the optimal compensation obtained at  $T = 0.4 E_R$  ( $T = 10.1t$ ) and  $T = 0.2 E_R$  ( $T = 5.1t$ ) in Figs. 17a and 17b respectively. With our current setup and optimal compensation we cannot run the LDA at temperatures below  $T = 5.1t$ . The sample extends so much into the lattice beams that the local  $T/t$  at the edge goes down to  $T/t = 1.5$  which is right at the limit of validity of the HTSE.

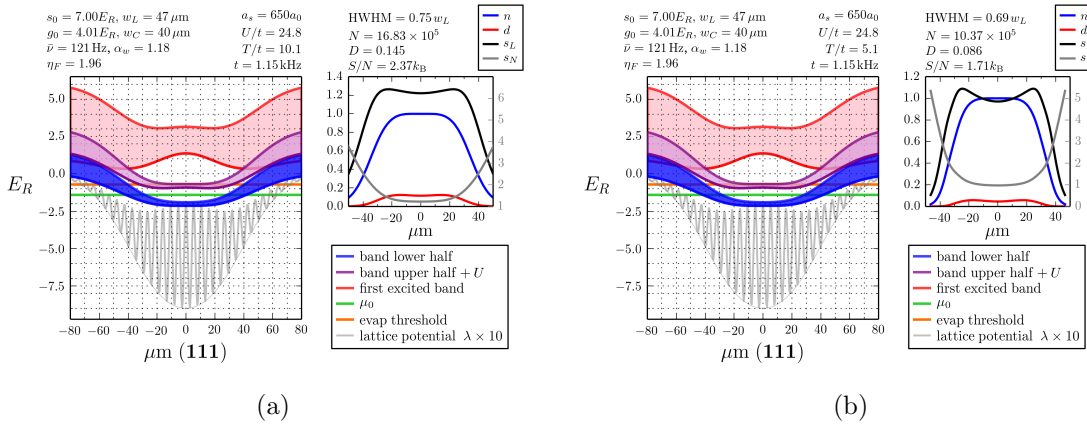


Figure 17

- In our current Bragg spectroscopy experiments we use  $N = 200,000$  atoms, so for our beam waists we have to reduce the compensation in order to achieve a density of one atom per site at the center. The LDA result for our current atom number and potential is shown for  $T = 0.2 E_R$  ( $T/t = 5.1$ ) and  $T = 0.12 E_R$  ( $T/t = 3$ ) in Figs. 18a and 18b respectively. SAY SOMETHING HERE ABOUT ETAF FOR THIS SETUP ALSO COMPARED TO ETAF IN THE SETUP WITH OPTIMAL COMPENSATION.

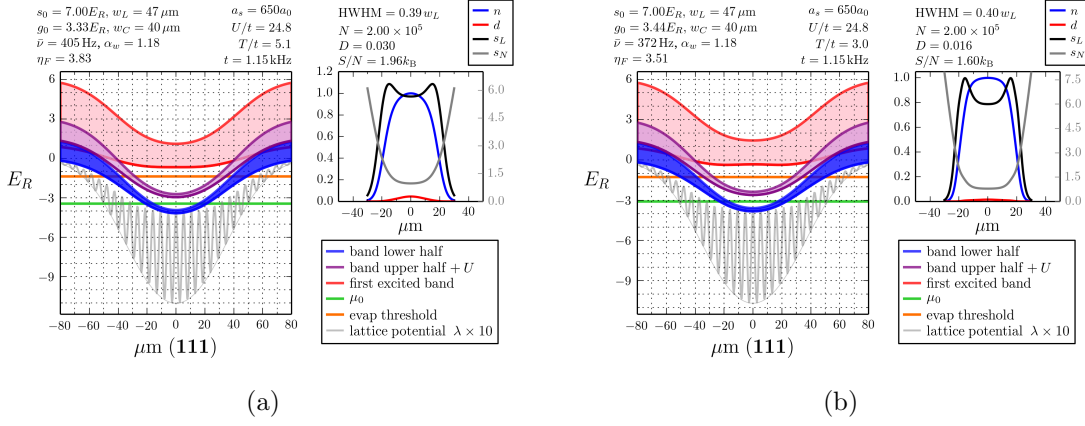


Figure 18

- In Fig. 19 we show the result for a uniform lattice and harmonic confinement, setting  $N = 200,000$  and  $n = 1$  at the center at a temperature  $T = 0.12 E_R$ . By comparing  $\eta_F$  and  $S/N$  to our current setup we can see that in the uniform lattice the situation for evaporation is much less favorable ( $\eta_F \approx 20$ ) but as far as entropy redistribution the situations are very similar ( $S/N \approx 1.6 k_B$  for 200,00 atoms).

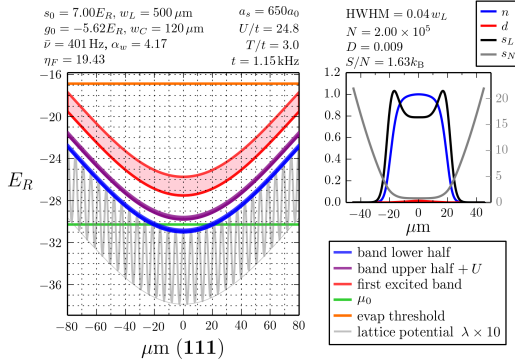


Figure 19

- Next we show the proposed scenario for our future implementation. We use a lattice beam waist  $w_L = 68 \mu\text{m}$ . With compensation beam waists in the range  $68 \mu\text{m} < w_C < 75 \mu\text{m}$ , that is around  $\alpha_w = 0.96$ , we can make samples that have good  $\eta_F$  and  $S/N$  characteristics. Additinally for these values of  $\alpha_w$  the resulting sample occupies a small fraction of the beam waist such that the lattice can be locked to a depth of up to  $\approx 30 E_R$ . The choice of  $w_L$  sets the scale for the atom number, which can be between 200,000 and 450,000 atoms in this range. Results are shown in Figs. 20a to 20c.

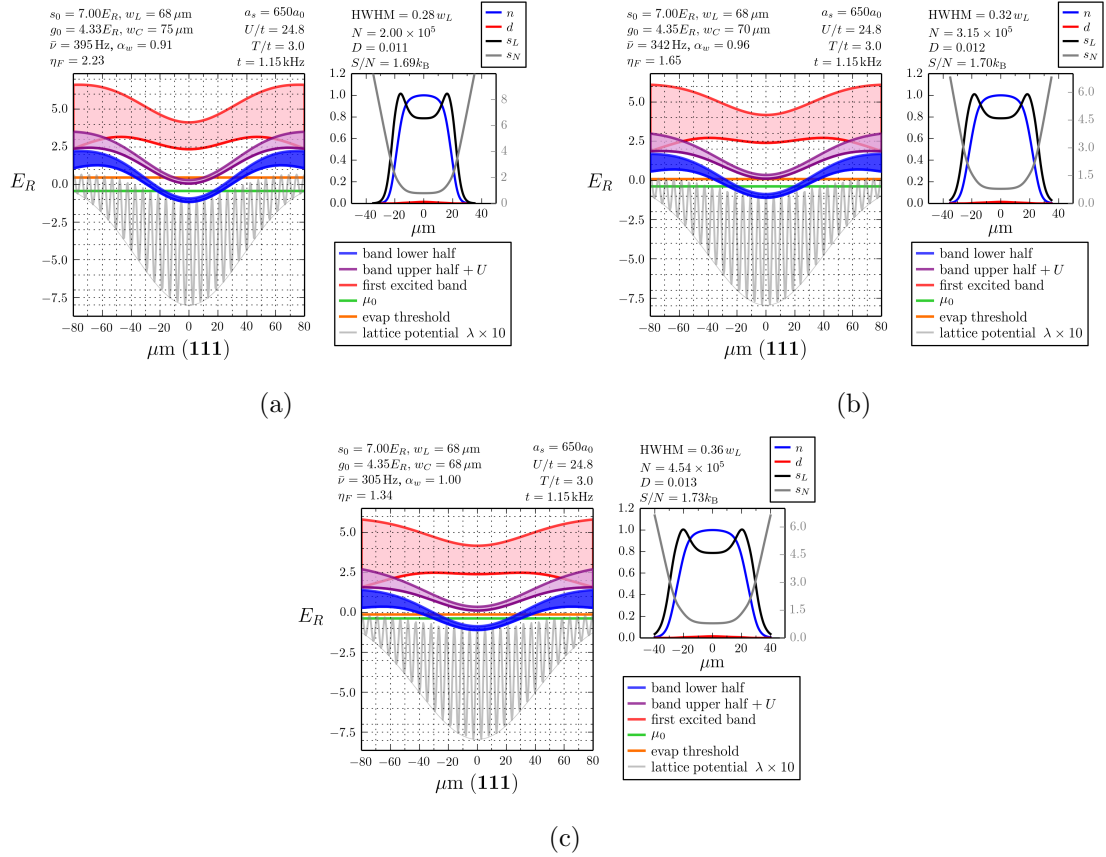


Figure 20

The profiles that are shown in Fig. ?? are calculated at a temperature  $T = 1.8t$ , which is near the lowest temperature value accessible with the HTSE. The chemical potential, measured from the lowest energy level available to the system (the bottom of the band) is set to  $\mu = 6t + U/2$  to guarantee half-filling at the center.<sup>4</sup> We used a value of  $U = 24.9t$ , given by the scattering length, which is set at  $650a_0$ .

Plugging in these values we obtain  $\mu \approx 18t$  or  $T/\mu \approx 1.8/18 = 0.1$ . When the temperature is so low, one can safely assume that  $\mu \approx E_F$ , so this system would have  $T/T_F = 0.06$  at an overall entropy per particle of  $S/N = 1.94k_B$ . If the sample was obtained by ramping up the lattice adiabatically starting from a harmonic trap, then the initial entropy in the harmonic trap should also be  $1.94k_B$ . In the harmonic trap this corresponds to  $T/T_F = S/(\pi^2 N) \approx 0.2$ .

We conclude from these rough estimates that as the sample gets loaded into the lattice it gets adiabatically cooled, its value of  $T/T_F$  is reduced. This is in contrast with the result obtained in [8] where it was concluded that loading a gas adiabatically from a harmonic trap to a deep optical lattice would adiabatically heat the gas. In this case we are considering interactions and not neglecting the width of the lowest band. Our observation that the gas is adiabatically cooled as it is loaded into the lattice are consistent with the results from [5].

(NOTE: I NEED TO ASK THEREZA ABOUT THESE REMARKS TO CHECK THAT I AM NOT MAKING A MISTAKE.

The main question is whether it is ok to take  $\mu = E_F$  since  $\mu$  is in the Mott gap. Should one take  $E_F = 12t$  in that case, since the top of the band is the largest energy state that could potentially be occupied?? )

#### 4.3.1 Enlarging the Mott state

In this section we consider our experimental setup ( $w_L = 47\text{ }\mu\text{m}$ ,  $w_C = 40\text{ }\mu\text{m}$ ) and we vary the amount of compensation. What we find is that if no compensation is used, then the number of atoms has to be very small in order to achieve half-filling at the center. On the other hand, when using compensation one can still hold a large number of atoms and maintain half-filling. This leads to the concept of enlarging the Mott state (or Néel state if your temperature is low enough) which can be a very dramatic effect as was shown in the paper by Mathy, Huse and Hulet [4].

The effect of enlarging the Mott state is shown in Fig. 21, where we show the relationship between atom number and compensation when the filling is set to  $n = 1$  at the center of the cloud. This figure also shows the profile plots for no compensation and a compensation of  $3.05 E_R$ , in order to illustrate how the Mott plateau in the density profile is enlarged for larger compensation.

From what was discussed in §?? we see that it is also possible to reach a large Mott plateau for  $N = 350,000$  and without compensation beams: you just need to have larger lattice beam waists. As we saw there, the advantage of realizing the large Mott plateau with small lattice beam waists and compensating beams is that this system has a larger entropy capacity than the large-beam-waist-uncompensated counterpart.

In addition to this entropy capacity advantage, the small-beam-waist-compensated setup offers the possibility of evaporative cooling since the chemical potential comes much closer to the energy threshold for an atom escaping along one of the lattice beams. We will address this point in the following section.

---

<sup>4</sup>The  $6t$  here is half the bandwidth. Note that in typical treatments the chemical potential is always measured from the center of the lowest band, so the  $6t$  will be omitted. In that case the chemical potential associated with half-filling Will be  $U/2$ . Some treatments even shift the zero of energy by  $U/2$  so that half filling occurs nominally at  $\mu=0$  regardless of  $U$ .

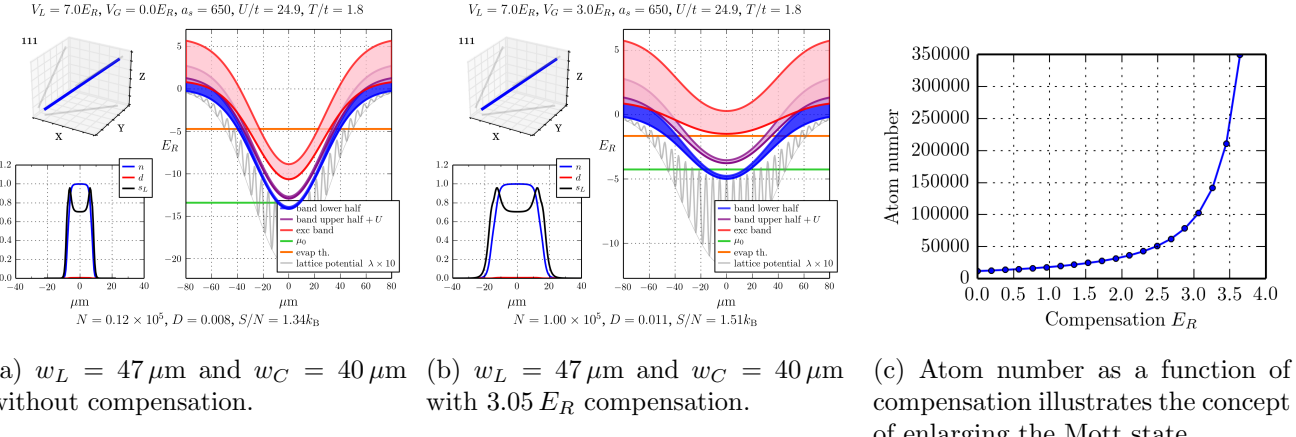


Figure 21: Illustrating the idea of enlarging the Mott state.

## 5 Evaporative cooling in a lattice

If we refer back to Fig. ?? we can see that on the energy landscape plot we used an orange line to indicate the evaporation threshold, that is the energy necessary for an atom to escape along one of the lattice beams. Comparing the two cases one sees that the small beam waist compensated case has a global chemical potential (green line) that is much closer to the evaporation threshold.

When evaporative cooling a thermal gas of atoms, one considers the parameter  $\eta = U_{\text{trap}}/k_B T$ , where  $U_{\text{trap}}$  is the energy threshold for a particle leaving the trap (i.e. the trap depth) and  $T$  is the temperature of the gas. The evaporation rate is suppressed by a factor  $\exp(-\eta)$  where typically  $\eta \sim 10$  and, as the gas cools down, the trap depth is reduced to force further evaporation [9].

For a deeply degenerate Fermi gas,  $T \ll T_F$ , the evaporation rate is given by [9].

$$\Gamma_{\text{evap}} \propto \gamma_{\text{coll}} \frac{T}{T_F} \exp \left[ -\frac{U_{\text{trap}} - k_B T_F}{k_B T} \right] \quad (27)$$

where  $\gamma_{\text{coll}}$  is the classical collision rate evaluated at the Fermi surface. This can also be written as

$$\Gamma_{\text{evap}} \propto \gamma_{\text{coll}} \frac{T}{T_F} \exp \left[ \frac{1}{T/T_F} \right] \exp \left[ -\frac{1}{T/T_F} \left( \frac{U_{\text{trap}}}{k_B T_F} \right) \right] \quad (28)$$

We define  $\eta_F \equiv U_{\text{trap}}/k_B T_F$  and observe that

$$\Gamma_{\text{evap}} \propto \gamma_{\text{coll}} \frac{T}{T_F} \exp \left[ -\frac{\eta_F - 1}{T/T_F} \right] \quad (29)$$

For the deeply degenerate gas, the  $\eta$  factor which determines the exponential suppression of the evaporation due to the trap depth is effectively

$$\eta = \frac{\eta_F - 1}{T/T_F} \quad (30)$$

Notice that the evaporation rate is additionally suppressed by a factor  $T/T_F$  due to Pauli blocking of one of the final states of a collision, which occurs for  $T \ll T_F$  [9].

We start by considering a red-detuned lattice with no extra confinement or compensation. We set

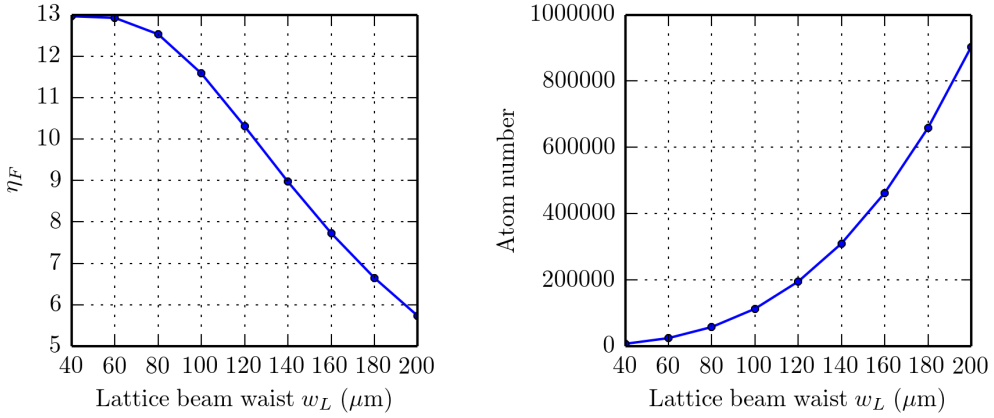


Figure 22:  $\eta_F$ , an indicator of the exponential suppression of evaporation is shown as a function of lattice beam waist for a red-detuned lattice without any extra confinement or compensation. To determine  $\eta_F$  the number of atoms is adjusted such that filling is  $n = 1$  at the center. The required number is shown on the right.

$n = 1$  at the center of the sample and vary the waist of the lattice beams. From our knowledge of the potentials we can determine  $U_{\text{trap}}$ , which in this case is the energy required for an atom to escape along one of the lattice beams. At a temperature of  $T = 1.8t$  we can make the approximation  $k_B T_F \approx \mu$ , where  $\mu$  is the global chemical potential. Figure 22 shows  $\eta_F$  as a function of lattice beam waist, and also shows the number of atoms required to achieve half-filling.

In our experiment we can produce cold samples with  $\sim 350,000$  atoms. As can be seen in Fig. 22 (and also was already shown in Fig. ??), using a beam waist of  $146\ \mu\text{m}$  would produce the confinement necessary to reach half-filling at the center with  $N = 350,000$ . The flip side of this is that, for that beam waist  $\eta_F$  would be  $\approx 8.5$ , which for  $T/T_F = 0.1$  means that the rate of evaporation would be suppressed by

$$\frac{T}{T_F} \exp \left[ -\frac{\eta_F - 1}{T/T_F} \right] \equiv \xi_{\text{evap}} \approx 10^{-34} \quad (31)$$

Going back to our current setup, which has  $w_L = 47\ \mu\text{m}$  and  $w_C = 40\ \mu\text{m}$ , with 350,000 atoms; we can achieve half filling if we use  $3.64E_R$  of compensation. This yields  $\eta_F \approx 2.95$ . This is a lot better than the large-beam-waist-uncompensated case, however the suppression factor for the rate of evaporative cooling is still very small. For our current setup it would be

$$\xi_{\text{evap}} = 3.4 \times 10^{-10} \quad (32)$$

Under typical evaporation conditions  $\eta = 10$ , and for a non-degenerate sample we have

$$\xi_{\text{evap}} = e^{-10} = 4.5 \times 10^{-5} \quad (33)$$

We conclude that our current setup would have an evaporation rate **five orders of magnitude smaller** compared to the typical evaporative cooling rate for a thermal gas (given the same rate of elastic collisions  $\gamma_{\text{coll}}$ ). In addition, in order to get a more realistic estimate we would need to incorporate the implications of the chemical potential being in a gapped region of the spectrum (for half-filling the chemical potential is at the center of the Mott gap) which should further reduce the evaporation rate.

We now explore the entire parameter space, where we allow the lattice and compensation beam waists to vary. We set the chemical potential so that  $n = 1$  at the center of the sample, we do this because

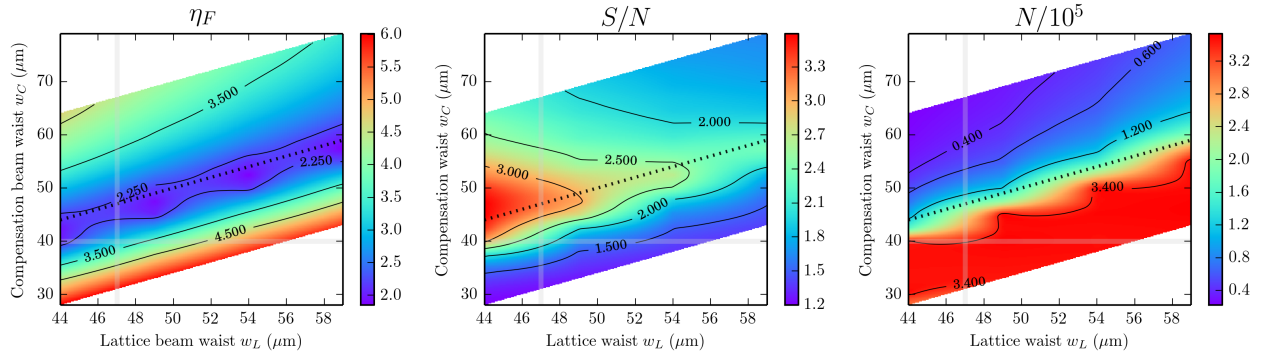


Figure 23:  $\eta_F$  and  $S/N$  and  $N$  are plotted for various lattice and compensation beam waists. The filling is set to  $n = 1$  at the center. The compensation depth is adjusted so that  $N = 350,000$  if it is possible, otherwise it is set to maximize the atom number without spilling any atoms from the trap or creating a Mexican hat at the center of the potential. The dotted line in the plots corresponds to  $w_L = w_C$ . The current values of our experimental setup are shown as gray lines, such that the intersection between these two gray lines represents our current conditions.

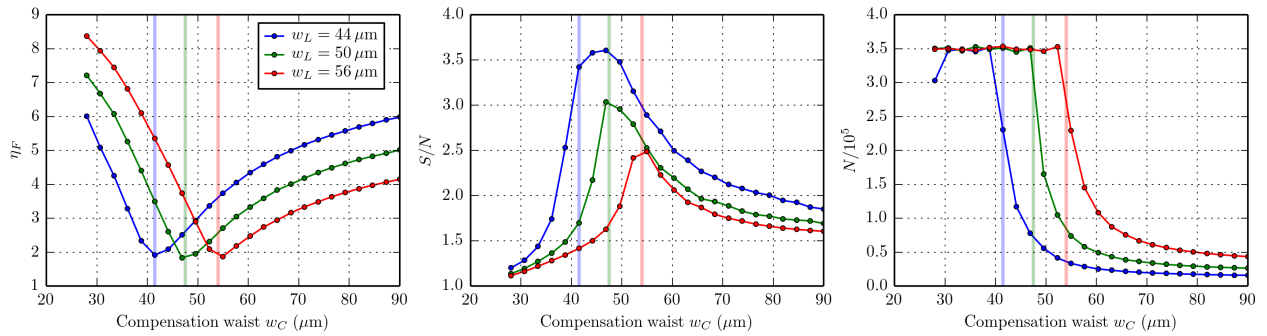


Figure 24:  $\eta_F$ ,  $S/N$ , and  $N$  as a function of  $w_C$  for various values of  $w_L$ .

half-filling is a prerequisite to achieve Mott or Néel states. We attempt to find a compensation such that  $N = 350,000$  atoms. For some values of the beam waists that is not possible because it would lead to either spilling atoms from the trap<sup>5</sup> or to the creation of a negative curvature in the confinement at the center of our sample<sup>6</sup>.

The results of the exploration of the beam waist parameter space are shown in Fig. 23. The main points that stand out are

- An optimal value of  $\eta_F$  is achieved for  $w_L \approx w_C$ .
- At  $w_L \approx w_C$ , smaller beam waists give better entropy capacity
- The atom number can only reach 350,000 if  $w_C < w_L$ , such as in our current setup. Otherwise the atom number is limited, being smaller for larger  $w_C$ .

To get another look at the results, on Fig. 24 we plot  $\eta_F$ ,  $S/N$ , and  $N$  as a function of  $w_C$  for three different values of  $w_L$ . The evaporation factor is optimized for nearly equal beam waists and the entropy capacity also peaks up around there. Given this observation, we now set  $w_L = w_C$  and vary both together to see if it is favorable to make smaller or larger beam waists. This is shown in Fig. 25. The main observations are:

<sup>5</sup>In cases when  $w_C > w_L$ .

<sup>6</sup>In cases when  $w_C < w_L$ . We also refer to this as making a donut

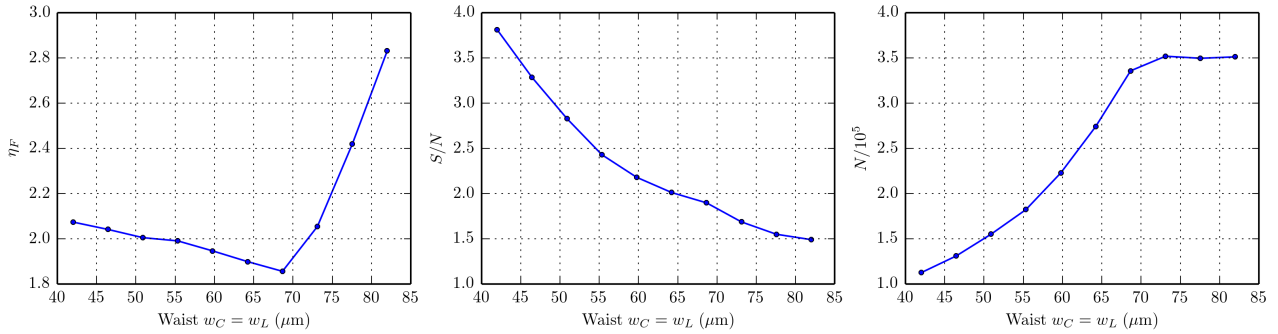


Figure 25:  $\eta_F$  and  $S/N$  as a function of beam waist for  $w_L = w_C$ . Results are shown for various atom numbers.

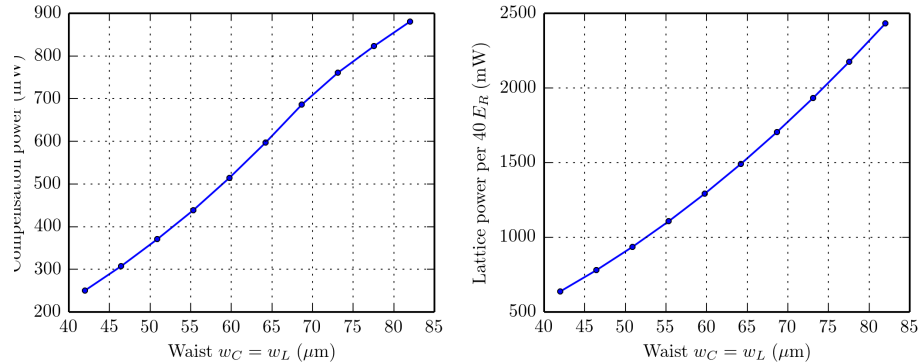


Figure 26: Compensation power required to compensate a  $7 E_R$  lattice and lattice powered required to achieve a  $40 E_R$  lattice depth.

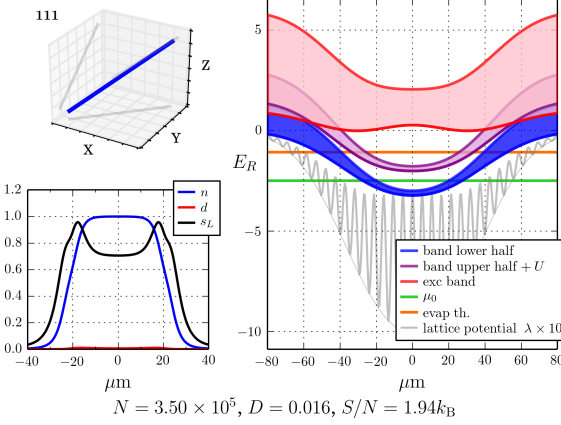
- For beam waists up to  $\approx 68 \mu\text{m}$  one can keep getting lower  $\eta_F$  by making the beam waists larger. This trend would continue if we had an unlimited number of atoms, however beyond  $\approx 68 \mu\text{m}$  the number of atoms required to fill the trap goes above our cap of 350,000 atoms.
- For larger beam waists the entropy capacity is always lower, so the choice of beam waist will be a compromise between  $\eta_F$  and the entropy capacity.

The results shown in Figs. 25, 24 show that it is desirable to have equal lattice and compensation beam waists. The choice of their value is a compromise between the achievable  $\eta_F$  and the entropy capacity, given by  $S/N$ . Another important experimental constraint is the available of power at the lattice and compensation wavelengths, which is a bigger issue for larger beam waists. In that case larger power is necessary to achieve the required potential depths. The compensation power needed to compensate a  $7 E_R$  lattice and the lattice power needed to make a  $40 E_R$  deep lattice<sup>7</sup> are shown in Fig. 26. With this in mind and our available powers we can safely realize any choice of beam waists below  $65 \mu\text{m}$ .

To fully exploit the atom number that we can produce in our experiment our opinion is to go to the larger lattice beam waists, so we recommend values of  $w_L = w_C = 65 \mu\text{m}$ . These proposed parameters would change the evaporation factor and entropy capacity and number capacity of our setup according to the following table:

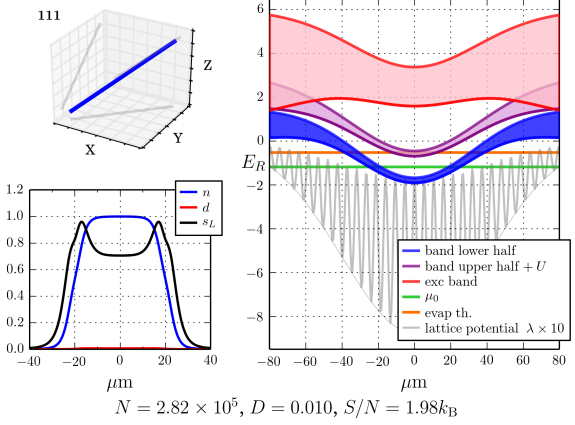
<sup>7</sup>If we want to freeze out tunneling in the lattice we required depths as large as  $40 E_R$  where the tunneling rate goes down to 3 Hz. We currently “lock” the lattice at  $20 E_R$  for our Bragg scattering measurements. At  $20 E_R$  the tunneling rate is 72 Hz. This is good enough for Bragg scattering, but not good enough for measurements that take longer, such as associating through the narrow Feshbach resonance to measure double occupancies.

$$V_L = 7.0E_R, V_G = 3.6E_R, a_s = 650, U/t = 24.9, T/t = 1.8$$



(a)  $w_L = 47 \mu\text{m}$  and  $w_C = 40 \mu\text{m}$ . Compensation is chosen so that unit filling is achieved at the center for an atom number of 350,000.

$$V_L = 7.0E_R, V_G = 4.1E_R, a_s = 650, U/t = 24.9, T/t = 1.8$$



(b)  $w_L = 65 \mu\text{m}$  and  $w_C = 65 \mu\text{m}$ . Atom number maxes out at 284,000 atoms.

Figure 27: Full trap profiles of band structure and thermodynamic quantities for our current setup and the proposed setup with equal beam waists.

	$w_L (\mu\text{m})$	$w_C (\mu\text{m})$	$\eta_F$	$\xi_{\text{evap}}$	$S/N$
Current setup	47	40	2.95	$3.4 \times 10^{-10}$	1.94
Proposed change	65	65	1.52	$1.36 \times 10^{-5}$	1.99

We see that for the optimal beam waist ratio a value of  $\xi_{\text{evap}} \sim 10^{-5}$  may be reached that could lead to reasonable rates of evaporation in the lattice. A comparison of our current setup and this proposed scenario is shown in Fig. 27.

## 6 Conclusions

## References

- [1] I. Bloch and W. Zwerger, “Many-body physics with ultracold gases,” *Reviews of Modern Physics* **80**, 885–964 (2008).
- [2] U. Schneider, Ph.D. thesis, Johannes Gutenberg - Universitat in Mainz, 2010.
- [3] R. Jördens, Ph.D. thesis, ETH Zürich, 2010.
- [4] C. J. M. Mathy, D. a. Huse, and R. G. Hulet, “Enlarging and cooling the Néel state in an optical lattice,” *Physical Review A* **86**, 023606 (2012).
- [5] T. Paiva, Y. L. Loh, M. Randeria, R. T. Scalettar, and N. Trivedi, “Fermions in 3D Optical Lattices: Cooling Protocol to Obtain Antiferromagnetism,” *Physical Review Letters* **107**, 086401 (2011).
- [6] S. Fuchs, E. Gull, L. Pollet, E. Buровски, E. Kozik, T. Pruschke, and M. Troyer, “Thermodynamics of the 3D Hubbard Model on Approaching the Néel Transition,” *Physical Review Letters* **106**, 030401 (2011).
- [7] J. Henderson, J. Oitmaa, and M. Ashley, “High-temperature expansion for the single-band Hubbard model,” *Physical Review B* **46**, 6328–6337 (1992).
- [8] M. Köhl, “Thermometry of fermionic atoms in an optical lattice,” *Physical Review A* **73**, 031601 (2006).
- [9] K. OHara, M. Gehm, S. Granade, and J. Thomas, “Scaling laws for evaporative cooling in time-dependent optical traps,” *Physical Review A* **64**, 051403 (2001).